ANALYZING THE MIXING DYNAMICS OF A TUMBLING BIN BLENDER USING DISCRETE ELEMENT MODELING

BY SUBHODH KUMAR KARKALA

A thesis submitted to the

Graduate School—New Brunswick

Rutgers, The State University of New Jersey

in partial fulfillment of the requirements

for the degree of

Masters of Science

Graduate Program in Chemical and Biochemical Engineering

Written under the direction of

Dr. Rohit Ramachandran

and approved by

_____

_____

_____

_____

New Brunswick, New Jersey

May, 2015

ABSTRACT OF THE THESIS

Analyzing the Mixing Dynamics of a Tumbling Bin Blender using Discrete Element Modeling

by Subhodh Kumar Karkala

Thesis Director: Dr. Rohit Ramachandran

Powder mixing is a critical step in pharmaceutical processes as it determines the final tablet composition. In this study a discrete element model (DEM) has been developed for an industrial scale tumbling bin blender in which three different materials are blended together. The dynamics of the mixing have been evaluated with the analysis of critical quality attributes (CQAs) such as relative standard deviation (RSD) and segregation intensity. This model has been developed and calibrated using an experimental setup in which the blend composition is monitored through a near-infrared range (NIR) probe mounted on the blender lid. The final blend quality is judged on the basis of measurements only at the lid in the experimental setup. However, the model has been used to study the quality of mixing in different locations inside the blender. The model is able identify poorly mixed zones and can be used to investigate other potential locations for the NIR probe. The effect of key process parameters (i.e. blender RPM and loading order of materials) on the quality of mixing has also been studied.

Acknowledgements

I would like to thank Dr. Rohit Ramachandran for giving me the oppurtunity to be part of his research group and allowing me to work on intersting projects. I would like to thank Dr. Bejamin Glasser and Dr. Marianthi Ierapetritou for being part of my thesis defense committee. I would also like to thank the Janssen Pharmaceuticals, Inc. of Johnson & Johnson for funding this project.

I would like to thank my family for their encouragement and support over the years. I am privileged to have them. This work would also not have been possible without the guidance and support of my mentor, Maitraye. Her patience and time in helping me in all of my projects is greatly appreciated. I would also like to thank Abhinav for all his help during these two years. Together, the two of them have had significant influence on how my graduate studies at Rutgers has shaped. I would also like to thank Savitha for her assistance in this project. Finally, I would like to thank all my friends from India who motivated me, guided me and helped me achieve this milestone.

Table of Contents

Abstract ii

Acknowledgements iii

List of Tables vi

List of Figures vii

1. Introduction and Objectives 1

1.0.1. Motivation 4

1.0.2. Objectives 4

2. Discrete Element Model 6

3. Mathematical Model Development 11

3.1. Experimental Setup 11

3.2. Geometry and Calibration of DEM Parameters 12

3.2.1. Particle Scale-up Procedure 12

3.2.2. Calibration of interaction parameters 14

3.3. Final DEM Input Parameters 15

4. Results and Discussion 17

4.1. Discretization of blender geometry 17

4.2. Comparison of Overall RSD composition with Layer-4 RSD 19

4.3. Segregation Intensity Comparison 21

4.4. Identification of Poor Mixing Zones 22

4.5. Proposed sampling sites for determining RSD 27
4.6. Reducing Segregation Intensity of Extra Granular Phase 28
4.7. Effect of Critical process parameters 28

5. Conclusions and Future work 33

References 35

List of Tables

3.1. Experimental set-up 11

3.2. DEM simulation parameters 16

List of Figures

2.1. Flow diagram of the working principle of DEM 10

3.1. Pictorial representation of the bin blender 13

4.1. Discretization of the blender into different zones (grid bins) 18

4.2. Layer-wise representation of the grid bins in cartesian system 19

4.3. Comparison of RSD between layer 4 and the overall RSD for (a) API 1 (b) API 2 (c) Extra granular phase 20

4.4. Intensity of segregation vs number of revolutions 22

4.5. Superpotent and Subpotent regions in the mixing of API 1 represented as (a) Cartesian grid system (b) 3D representation 24

4.6. Superpotent and Subpotent regions in the mixing of API 2 represented as (a) Cartesian grid system (b) 3D representation 25

4.7. Superpotent and Subpotent regions in the mixing of Extra Granular Phase represented as (a) Cartesian grid system (b) 3D representation . 26

4.8. Comparison of Overall RSD with Layer-4 and Wall hotspots for (a) API 1 (b) API 2 30

4.9. Variation of segregation intensity of Extra Granular Phase with change in processing conditions 31

4.10. Loading order of the materials 31

4.11. Variation of RSD of API 1 with change in processing condition 32

Chapter 1
Introduction and Objectives

Powder mixing combines two or more materials into a blended mixture and is an important unit operation in several industries (e.g., food, pharmaceutical, chemical etc.). A key attribute of powder mixing is the blend uniformity. As the blender output is processed further in downstream units, the blend uniformity has a significant influence on the quality of the final product. Hence the performance of the mixing operation is critical to the operational efficiency of these industries [1].

A variety of blenders are available for processing powdered materials in the industry. The application of these blenders depends on the properties of materials being mixed. The tumbling bin blender is a batch mixer used to blend granular materials together. They are commonly used in pharmaceutical industries as they provide safety in operations and convenience in handling [2]. However, due to the presence of multiple flow regimes in a tumbling blender, it is important to understand the process dynamics in detail. Moreover, as the pharmaceutical industries often have to deal with fine powders which have poor flowability and tend to segregate, mixing them efficiently may become quite challenging [3].

In general, the powder flow processes are erratic and have an inherent variability associated with it. Hence, various flow analyzing methods (experimental or modeling) are required to obtain a good prediction of their behavior. Enabling the use of process systems engineering (PSE) tools could prove very beneficial in understanding unit operations that process powered materials in pharmaceutical

industries. The various PSE tools which can be used for process development are predictive models, flexibility and feasibility analysis, steady state and dynamic optimization, sensitivity analysis and controller design [4]. Process models are mathematical representations of any system. They are developed based on experimental observations and physical principles and aid in providing a better understanding of the process. A calibrated model can also be used as a predictive tool. Thus the various modeling techniques and simulation tools can prove to be more resource and time saving alternatives when compared to other experimental methods for process design and optimization analysis.

Pharmaceutical industries have to abide by stringent quality norms set by the regulatory authorities (e.g. United States Food and Drug Administration (FDA)). Good product quality can be realized by designing robust manufacturing processes, incorporating thorough process knowledge. Managing and retaining an explicit process knowledge throughout the product life-cycle is an important aspect quality management system, as stated in ICH-Q10 [5]. Thus these industries are implementing more robust and science based process design methodology to ensure retention of a detailed process knowledge and re-assess the various product quality risks and uncertainties associated with it.

A detailed mathematical model that is validated, well-tuned and calibrated can be used as an efficient tool for pharmaceutical manufacturing process development studies [6], which will help to outline the design space. Design space is defined as "the multidimensional combination and interaction of input variables (e.g., material attributes) and process parameters that have been demonstrated to provide assurance of quality" (ICH: Q8 (R2)). A mixing operation involves a large parametric space which consists of the processing parameters (i.e. blender RPM, fill volume, loading pattern etc.), equipment design, material properties etc. [2, 7]. A process may consist of several input parameters, but only some are highly sensitive and critical towards the optimal operational efficiency of the

process. Therefore, identifying the critical process parameters (CPPs) and understanding their effect on the process efficiency is an important step in establishing the design space and evaluating how effectively the process can withstand any parametric variability without a drop in product quality. The manufacturing steps implemented by the pharmaceutical industries must meet the GMP (Good manufacturing practices) guidelines to achieve high process efficiency and good product quality as outlined by the FDA. This will also allow the product quality to be built consistently in each and every step of the manufacturing process as per the QbD and PAT guidelines.

PAT has been defined as "a system for designing, analyzing, and controlling manufacturing through timely measurements of critical quality and performance attributes of raw and in-process materials and processes with the goal of ensuring final product quality" (ICH: Q8 (R2)). It recommends implementation of measurement and control tools for the CPPs and material properties in the process so as to achieve product of desired quality. The process variables and parameters must be maintained within the acceptable limits as any deviation may lead to production of inferior quality product and also result in process failure which may have hazardous impact on the environment, health, safety etc. A mathematical model can also aid in the design and evaluation of an efficient control loop system based on the process understanding. In short, a process model can be used for virtual experimentation and can be a prerequisite for the design, analysis, control and optimization studies of a process.

Another important step in the design stage of a manufacturing process is the process risk analysis. Risk has been defined as "the combination of the probability of occurrence of harm and the severity of that harm" (ICH: Q9). It is necessary to formulate an effective risk management process which comprises of analyzing and assessing the risks associated with a process (i.e., environmental, health, safety etc.). A robust risk management process includes several steps which are

risk assessment (risk identification, risk analysis, risk evaluation), risk control (risk reduction, risk acceptance) followed by reviewing the outputs of the risk management process [8]. A good understanding of the potential risks will lead to reduction in prediction uncertainties and increase the sustainability of the process. As PSE tools can be used effectively to obtain the process knowledge, identify the CPPs, understand the inter-dependence of the CPPs, they can be an excellent source of evaluating the process risks followed by their application in optimization and sensitivity analysis and designing efficient control systems.

1.0.1 Motivation

Tumbling bin blenders are commonly used in pharmaceutical industries for the mixing of dry granular materials. Since mixing is a critical unit operation in these industries, modeling tools can prove useful to provide a detailed process understanding that is required for process design and optimization. Models can be used to for virtual experimentation and can help save resources by minimizing the experimental trials required. Hence, modeling tools will also help the pharmaceutical industries to attain a more sustainable position.

1.0.2 Objectives

In this work a mathematical model for an industrial batch bin blender has been presented and the mixing dynamics has been studied in terms of blend composition at different locations inside the blender, which has been further translated into RSD and intensity of segregation information. The model has been developed using discrete element methodology, which is a fundamental particle level modeling and simulation tool. It provides an excellent demonstration as how DEM (a model based technique) can be used as an effective tool to obtain a detailed process knowledge which can be further used in process design or troubleshooting

practical processing issues. In the actual experimental set-up, the NIR probe is used to monitor the blend composition, which is mounted on the lid of the blender. It performs a blend reading every time the bin is positioned with the lid down. The NIR is able to capture the blend composition near the lid region only. However, a model-based method can been used in order to evaluate the mixing in the entire blender. Thus the mixing efficiency can be studied in other locations as well (apart from the lid region). This will also help to identify other sampling locations.

The objectives of this study are listed below:

- Formulate a DEM model of an industrial scale tumbling bin blender.
- Study the mixing dynamics of the blender using the model based approach in terms of CQAs such as the RSD, segregation intensity and composition.
- Determine if the NIR measurements in the lid zone provide an accurate representation of the overall quality of mixing using the model.
- Evaluate poor mixing zones inside the blender and identify potential sampling sites with the help of the model
- Assess the sensitivity of the model to critical process parameters (i.e., RPM, fill volume and loading order).

Chapter 2
Discrete Element Model

A variety of modeling approaches are available in the literature that have been used to develop and study models for powder mixing processes. These include the Monte Carlo method, the DEM models, residence time distribution (RTD) models, population balance models, statistical models and hybrid models to name a few. Of these available approaches, DEM is one of the most fundamental modeling techniques used to simulate the behavior of powder in mixing processes. Powder systems consist of solid particles which are discrete entities and can interact with each other or the equipment boundary in different manner. DEM is often used to simulate powder flow as it treats the particles as discrete entities and is able to track the flow-field of individual particles. The mathematical formulation of DEM is derived from first-principles.

The mechanism used in DEM to track particle movements inside the system boundary is outlined in figure /refFig13. The geometry of the equipment is first created and the particles are simulated inside it. Next, DEM determines the contact or collisions between the particles. DEM then calculates the total force acting on the particles due to the particle-particle and particle-boundary contacts (contact forces) and other body forces (due to an external source; example: force of gravity). It then computes the acceleration or velocity using Newton's second law and updates the particle position based on the velocity information.

Two types of forces (which are normal pressure force and tangential frictional force), act on the particles due to contact. The contact forces are calculated

from the various contact models that are available (i.e., Hertzian normal contact force model, Cundall and Stack normal force model, J-K-R normal and adhesive force model for cohesive particles, Mindlin-Deresiewicz/Coulomb friction tangential force model etc.) [9]. In this work Hertzian normal contact force model and Mindlin-Deresiewicz tangential force model have been used as the DEM simulates free flowing non-cohesive powders. Hertzian normal contact force model assumes a non-linear spring-dashpot model and is applicable within elastic limits for spherical and smooth particles with continuous surface and undergoing non-conforming contact. As detailed by Kruggel-Emden et al. [10], particle-particle contact is detected between two spherical particles when the distance between their centers is less than the sum of their radii; and a particle-boundary contact is detected when the distance between the particle center and the boundary is less than the particle radius. However, a very small overlap (or deformation) may be allowed. As shown in equation (2.1), the total force ($\vec{F}$) acting on the particles is summation of the normal contact force($\vec{F_C^N}$), tangential/frictional contact force ($\vec{F_C^T}$) and body force ($\vec{F_B}$). In a bin blender model, the only body force acting may be due to gravity.

$$\vec{F} = \vec{F_C^N} + \vec{F_C^T} + \vec{F_B} \tag{2.1}$$

The acceleration of the particles is calculated from Newton's law $m\vec{a} = \vec{F}$, where m is the particle mass and $\vec{a}$ is the acceleration vector. The position of the particles is updated from Euler's equations of rotational motion as shown in equation (2.2) [11]. Here x, y and z are the spatial coordinates of the particle position, I is the moment of inertia, $\vec{\Omega}$ is the angular velocity vector and $\vec{\tau}$ is the torque.

$$I_{xx}\vec{\Omega}_x + (I_{zz} - I_{yy})\vec{\Omega}_z\vec{\Omega}_y = \vec{\tau}_x$$
$$I_{yy}\vec{\Omega}_y + (I_{xx} - I_{zz})\vec{\Omega}_x\vec{\Omega}_z = \vec{\tau}_y$$
$$I_{zz}\vec{\Omega}_z + (I_{yy} - I_{xx})\vec{\Omega}_y\vec{\Omega}_x = \vec{\tau}_z \tag{2.2}$$

The normal or tangential contact forces are calculated as $\vec{F_C} = -k\delta^{3/2} - \gamma\dot{\delta}\delta^{1/4}$. Here $\vec{F_C}$ is normal or tangential contact force, δ is the normal or tangential overlap, k is the stiffness coefficient factor, $\dot{\delta}$ is the rate of normal or tangential deformation and γ is the damping coefficient. The detailed expressions of these parameters have been given by Dubey et al. [11]. The stiffness coefficient controls the particle stiffness and is a function of the particle size and other material properties (i.e., Poisson's ratio and Young's modulus). The stiffness of a body can be defined as its ability to resist deformation when a force is applied on it. Fine tuning of the values of Poisson's ratio and Young's modulus is important because it decides the stiffness of the particles which on the other hand controls the particle deformation or overlap upon contact. It is suggested that the particle overlap be controlled so that the model stays within elastic limit [12].

Several modeling tools have been used in literature to study mixing. DEM has been used to investigate mixing of granular materials [13]; mixing behavior in a continuous mixer was investigated using compartment models [14]; markov chain modeling has been used to study powder mixing kinetics [15]; segregation and mixing were studied with the help of continuum modeling [16]; population balance modeling methodology was utilized to study continuous powder mixing [17] etc. DEM is an excellent tool to obtain fundamental particle level information which is not possible based on other modeling techniques which have been used to model powder systems. Several researchers have used DEM for studying powder mixing in different types of blenders (both batch and continuous mode of processing). For

example DEM has been used to study V-blender [18], conical blender [19], tote blender [20], rotating drums [21] and other continuous processing blenders [22]. DEM has also been coupled with other modeling tools for to improved process understanding. DEM has been combined with PBM (population balance models) and compartment models in order to formulate multi-scale frameworks which are able to store process dynamics information from macro, meso and micro scales. For example, Sen et al. developed a PBM-DEM framework for a continuous mixing process [24]; Portillo et al. developed hybrid DEM-compartment model for granular mixing [25]; Kumar et al. developed a DEM-compartment-PBM coupled model for a particle coating process [26].

In this work a case study on an industrial blender has been presented which demonstrates how DEM can be applied in a practical scenario to study mixing.

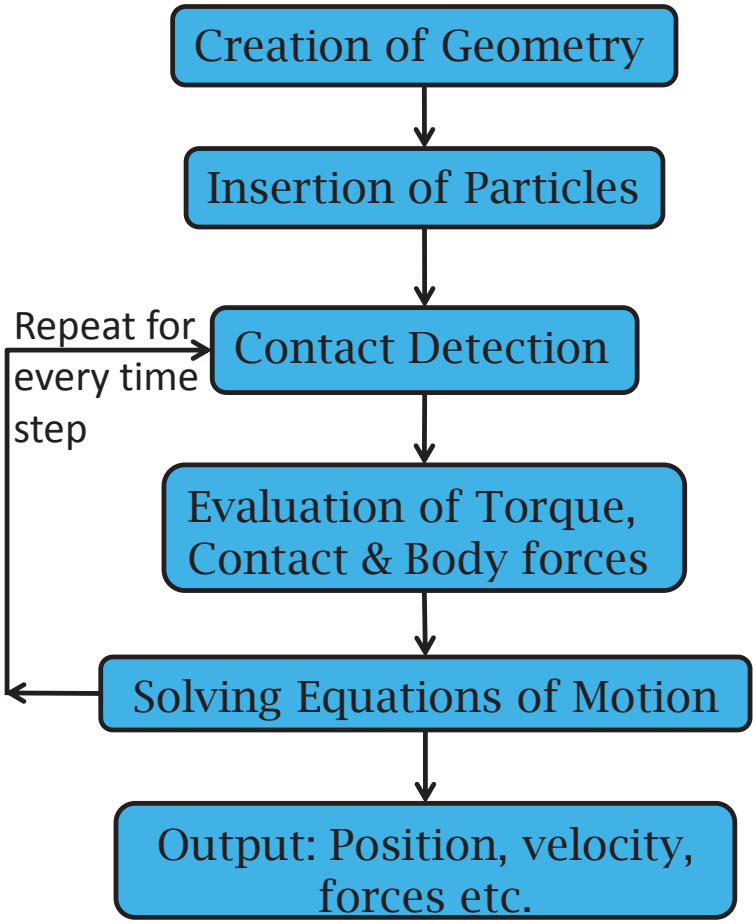

Figure 2.1: Flow diagram of the working principle of DEM

Chapter 3
Mathematical Model Development

In this section an overview of the procedure followed for model development has been presented. The experimental set-up has been described first. Next, the steps taken for calibrating the DEM input parameters (particle size, number of particles, shear modulus, Poisson's ratio, particle-particle and particle-wall coefficients of static and rolling friction, coefficient of restitution) have been explained. Lastly, the final simulation parameters have been presented.

3.1 Experimental Setup

The blender is a cylindrical vessel with a conical bottom. Three different types of materials have been mixed together in the blender. Two of which are active pharmaceutical ingredients (API 1 and API 2) and the third is the excipient and has been termed extra granular phase. Table 3.1 gives the physical properties (mean particle size, true density and angle of repose) of the different materials and the feed composition.

In the experimental studies, the material loading procedure is as follows: half of API 2 is loaded first into the bin followed by the entire mass of API 1, followed

Material type	**Mean Particle size** (μm)	**True Density** (g/cc)	**Angle of repose** (degree)
API 1	420	0.7159	45
API 2	401	0.6720	42
Extra granular phase	178.2	0.7316	61

Table 3.1: Experimental set-up

by the entire mass of the extra granular phase after which the remaining half of API 2 is loaded. The blender is operated at a speed of 6 RPM. The model input parameters have been determined by tuning and calibrating with respect to the experimental set-up.NIR data is collected every revolution after the first 30 revolutions are over. As mentioned previously, the NIR probe is located at the blender lid and the data is collected when the blender is in inverted position. The DEM study has been conducted on this simulation set-up and processing conditions.

3.2 Geometry and Calibration of DEM Parameters

The geometry of the bin blender has been shown in figure 3.1. This geometry has been developed using 3D-CAD (SolidWorks^{TM}) and has been built to scale. The DEM simulations have been performed in EDEM^{TM} (DEM Solutions).

3.2.1 Particle Scale-up Procedure

The particle size in the DEM simulation has been scaled up from the actual particle size. Realizing the actual particle size in DEM is not feasible. Billions of particles (with the actual particle size) will have to be created in order to fill the processing volume and this will make the model extremely computationally intensive as DEM tracks each individual particle across the space of the system. Scaling up the particle size will allow the same processing volume to be filled by lesser number of particles thereby increasing the simulation speed.

The total number of particles to be simulated and the scaled-up particle radius have been decided in a manner such that the fill volume/fill level and the mass of the batch matches with the experimental set-up. The composition of the feed has been also been kept the same as in the experimental setup. As there are three material types being mixed, therefore three particle types have been created in

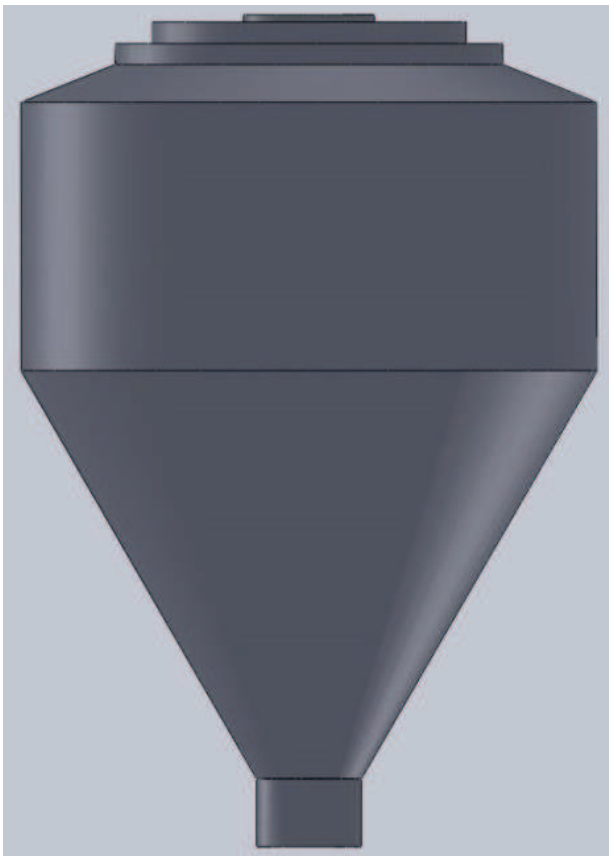

Figure 3.1: Pictorial representation of the bin blender

DEM and the properties of each have been calibrated (let 'i' represent the three different particle types).

The particles used for the DEM simulation have been scaled-up based on the actual mean particle size. First, the total number of particles (including all the three material types) that will be simulated in DEM has been fixed, N_{Total}. Total volume occupied by all the particles of type 'i' in feed is given as $V_i = \frac{m_i}{\rho_i}$, where ρ_i and m_i are the bulk density and total mass of all the particles of ith type (ρ_i and m_i are obtained from the experimental data). The size ratios of each particle type have been calculated with respect to the extra granular phase $S_i = \frac{R_i}{R_{extra\ granular\ phase}}$, where R_i is the actual mean radius (from experiment) of one particle of type 'i' (size ratio of the extra granular phase is 1). A porosity ϕ_i has been assigned to each particle type (based on experimental data) in order to

calculate the number of particles of individual components $N_i = \frac{V_i(1-\phi_i)}{v_i}$, where v_i is the volume of one particle of type 'i'. Let r_1 be the radius of the smallest particle type to be created in DEM. Replace v_i as $v_i = \frac{4}{3}\pi(S_i r_1)^3$ in the expression for N_i (i.e.,$N_i = \frac{V_i(1-\phi_i)}{\frac{4}{3}\pi(S_i r_1)^3}$) . If M is the number of components/particle types (M=3 in this case), then the scaled-up radius (or DEM radius) of one particle to be simulated is given as equation (3.1) (put the expression of N_i in the expression of N_{Total} and through algebraic manipulation obtain r_i).

$$N_{Total} = \Sigma_{i=1}^{M} N_i$$
$$r_1^3 = \frac{3}{4\pi N_{Total}} \Sigma_{i=1}^{M} \frac{V_i(1-\phi_i)}{S_i^3} \tag{3.1}$$

3.2.2 Calibration of interaction parameters

It should be noted that the particle size ratio and the weight ratio between the three raw material types have been maintained similar to the experimental set-up. Once the particle size has been decided for all the raw material types, the values of the other input parameters need to be determined. The other parameters which must be provided as inputs to the model are material density, shear modulus, Poisson's ratio and the interaction parameters (i.e., coefficient of static friction, coefficient of rolling friction and coefficient of restitution). The value of shear modulus and Poisson's ratio has been fine tuned so that at every time step, the maximum allowed value for particle-particle and particle-wall overlaps is 15% of the particle radius. The values of the interaction parameters have been fixed by calibrating them with respect to the experimentally obtained angle of repose. The angle of repose of any material is highly sensitive to the coefficients of static and rolling friction. A detailed analysis on calibration of DEM interaction parameters based on angle of repose has been given by Zhou et al. [27]. Several trial simulations have been run for each material type by varying the value of the interaction

parameters, such that the angle of repose obtained from the simulation can be matched with the experimental observation. In these simulations, particles have been created randomly inside a closed box followed by a gravitational settling process of about 5-10 s so that a stable packing is obtained. At the next instance the side and the top walls of the box are opened. The particles slide down until a stable pile is formed. The angle of repose has been determined from the surface profile of the pile.

3.3 Final DEM Input Parameters

The final set of simulation parameters (particle mean size, shear modulus, Poisson's ratio, coefficients of static and rolling friction and coefficient of restitution) have been presented in this section.

Table 3.2 gives the DEM particle diameter, number of particles and the interaction parameters used in the simulation. Here, μs_{pp}, μs_{pw}, μr_{pp} and μr_{pw} are the coefficient of static friction (particle-particle), coefficient of static friction (particle-wall), coefficient of rolling friction (particle-particle) and coefficient of rolling friction (particle-wall) respectively.

The coefficient of restitution has been kept at a low value of 0.01 as powder particles undergo inelastic collision [11]. The shear modulus and Poisson's ratio are 2 MPa and 0.33 respectively. The blender speed has been maintained at 6 RPM. A total of 200,000 particles have been simulated. This number has been chosen so that simulation completed in a reasonable amount of time using the computational resources available. The material loading order in the simulation has been maintained same as that mentioned in the experimental set-up section. The simulation has been run for a period of 502 seconds which is a total of 50 revolutions. The output data has been collected every five revolutions till first 30

revolutions. From 30 revolutions onwards, data has been collected for each revolution until 50 revolutions. This simulation has been termed as the base case. The base case has taken 22 days to simulate (for 502 seconds) on a 30 cores in an Intel Xeon (R) CPU @ 3.10 GHz with 128 GB RAM desktop computer.

Material type	**Particle diameter** (mm)	μs_{pp}	μs_{pw}	μr_{pp}	μr_{pw}
API 1	21.21	0.50	0.40	0.10	0.08
API 2	20.26	0.50	0.40	0.05	0.08
Extra granular phase	9.02	0.95	0.90	0.10	0.05

Table 3.2: DEM simulation parameters

Chapter 4
Results and Discussion

Several flow regimes may exist in a batch mixing process. These flow regimes could create zones that have different mixing efficiencies (i.e., differ in the composition and variability of the blend attributes). Therefore, it is important to investigate the mixing performance in different zones inside the blender. Such a study will also help to identify the poor mixing zones that may be present in the blender. Any unit operation is sensitive to certain process parameters and it has been shown in the previous studies that the mixing efficiency changes significantly with the change in the conditions of these process parameters [28]. In this study, mixing efficiency has been quantified by measuring the RSD and the intensity of segregation. The results shown in this section are from the model based study only and the same observations have to be experimentally verified.

4.1 Discretization of blender geometry

A Cartesian co-ordinate system has been used to discretize the blender into several zones. The geometry has been divided into four layers as shown in figure 4.1. Each layer has been further divided into 16 grid bins. As a result, the geometry has been divided into a total of 64 grid bins (4x4x4 in x, y and z direction respectively). Note that a grid bin represents a zone or location inside the blender.

The grid bin size has been decided such that there are adequate number of particles present in them to provide a good estimate of the composition and the variability. The bin size and hence the total number of bins has been varied and

RSD has been calculated by post processing the simulation across different time points. The final bin size has been chosen in the range where least change is observed in RSD in between the two bin sizes.

From the figure 4.1, it can be seen that certain grid bins contain no particles or very few particles. This is because the particles order themselves to form a slope inside the bin when it is inverted and also due to the fact that a Cartesian co-ordinate system has been considered in order to discretize a cylindrical vessel. Such bins have been excluded from the calculations so that unreliable results are not obtained.

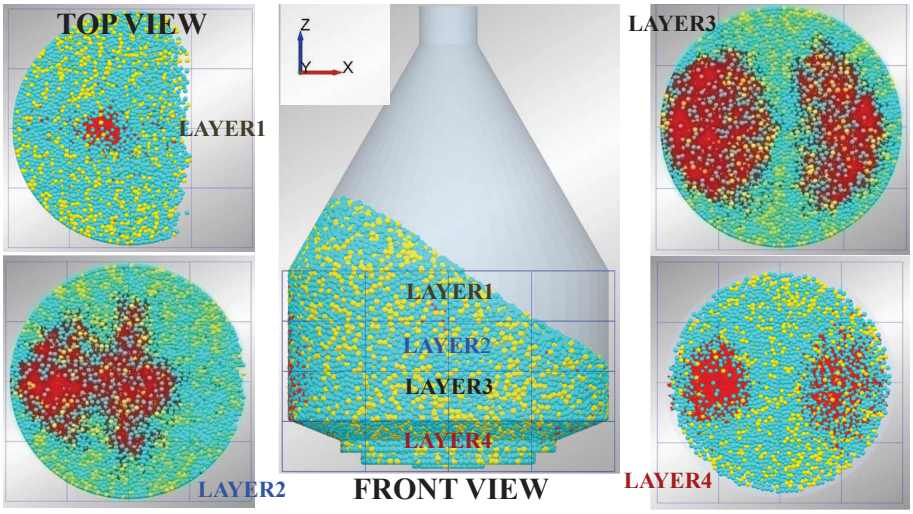

Figure 4.1: Discretization of the blender into different zones (grid bins)

Figure 4.2 presents the Cartesian grid bin representation of the four layers from the top view. Grid bins that have been excluded for calculation purposes have been marked green. In the experimental set-up, the NIR probe is present in the layer 4. Therefore, the probe is only able to capture the blend composition of grid bin 6, grid bin 7, grid bin 10 and grid bin 11 in layer 4. In the calculations involving these grid bins, the results of the first few revolutions have not been presented because at start up these values maybe unreliable in predicting the state of the system.

Figure 4.2: Layer-wise representation of the grid bins in cartesian system

4.2 Comparison of Overall RSD composition with Layer-4 RSD

Figure 4.3 shows the comparison between the overall RSD of each material type to their respective RSDs in the layer 4 as a function of number of revolutions. RSD has been determined based on equation (4.1) as shown below. RSD is a measure of the variation.

$$RSD = \frac{\sqrt{\frac{\sum_{i=1}^{i=M}(x_{avg}-x_i)^2}{M-1}}}{x_{avg}} \tag{4.1}$$

As mentioned earlier, the blender has been divided into several bins and samples for measurements have been collected from each of these bins apart from those excluded (as shown in figure 4.2). Here x_{avg} is the overall average fractional composition, x_i is the fractional composition at the ith bin and M is the total number of bins. Figure 4.3 a, b and c represent the comparison of RSD of API 1, API 2 and the extra granular phase respectively. The fluctuations present are inherent property of a DEM simulation because it is difficult to realize a perfect steady state in a powder system. As the powder particles can interact

with each other and the geometry wall in several different ways, based on the interaction parameters and contact angle etc., fluctuations in the output variables are often observed [24]. It can be seen from the plots that the current NIR probe which is located in the layer 4, is under estimating the overall variability in the mixture. There is a scope for identifying other sampling locations such that a better estimate of the overall mixture variability can be obtained.

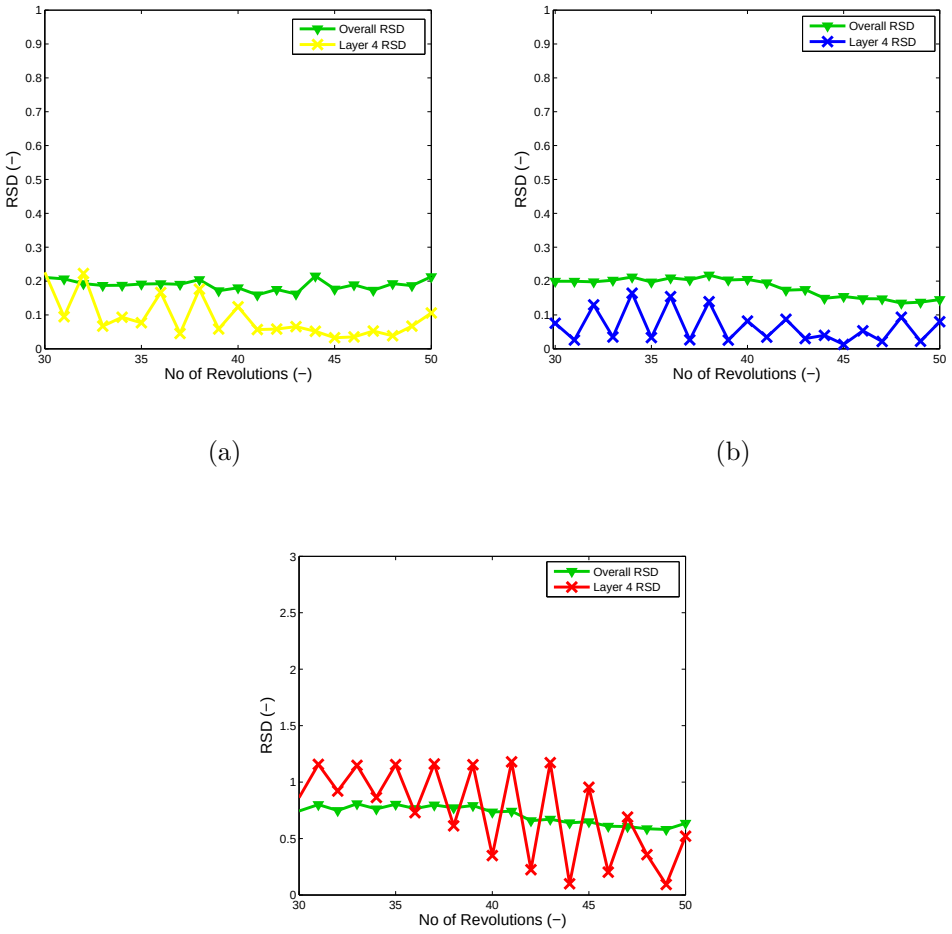

Figure 4.3: Comparison of RSD between layer 4 and the overall RSD for (a) API 1 (b) API 2 (c) Extra granular phase

4.3 Segregation Intensity Comparison

Segregation effect is often seen in powder handling operations as particles with different size and density often tend to form segregated layers thus deteriorating mixing performance. In the simulation of the blending process, three different materials with different particle sizes and densities are being mixed together. As a result, the likelihood of observing the segregation effect is high. In order to quantify the extent of segregation of the three material types, the intensity of segregation has been determined based on the formula [29] below:

$$I = \frac{\sum_{i=1}^{i=M}(x_{avg} - x_i)^2}{M x_{avg}(1 - x_{avg})} \tag{4.2}$$

As mentioned earlier, the blender has been divided into several bins and samples for measurements have been collected from each of these bins. Here I is the intensity of segregation, x_{avg} is the overall average fractional composition, x_i is the fractional composition at the ith bin and M is the total number of bins.

Figure 4.4 shows the intensity of segregation as a function of the number of revolutions for all the three particle types. Evidently, the segregation intensity of the extra granular phase is the highest. Particle sizes of API 1 and API 2 in the simulation are similar. The size ratio between these two particle types is 1:1.05. On the other hand, the particles of the extra granular phase are approximately 2.5 times smaller than the other two particles. This significant difference in size causes the extra granular phase to form a segregated layer which is mixing slower compared to the other two material types.

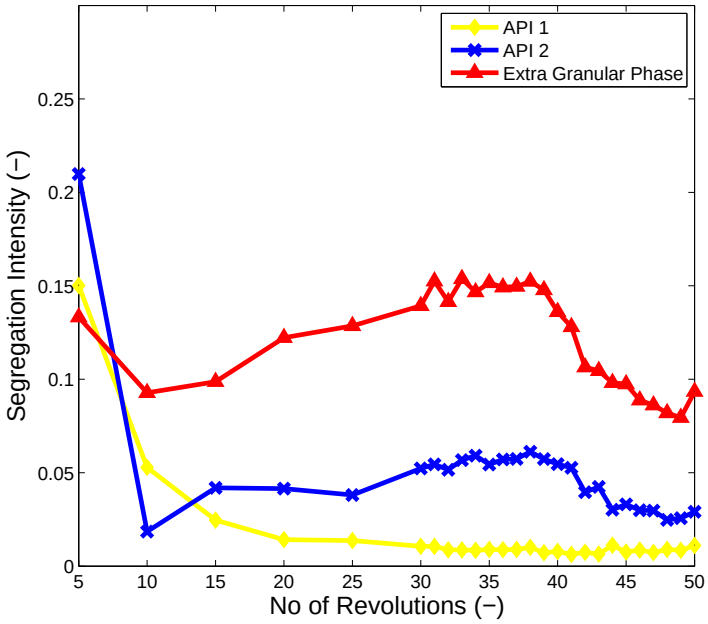

Figure 4.4: Intensity of segregation vs number of revolutions

4.4 Identification of Poor Mixing Zones

Another study has been conducted wherein the locations of poorly mixed regions inside the blender model have been ascertained. The grid bins with maximum and minimum fractional composition (with respect to the whole blender) have been identified at every revolution from 30 revolution onwards (i.e., from 30^{th} revolution to the 50^{th} - a total of 21 revolution points). If the occurrence of an extrema in a particular grid bin was more than three counts then that bin has been marked. The bins have been color coded with red representing superpotent regions and green representing subpotent regions.

Figures 4.5a and b show the superpotent and subpotent bin locations for API 1 in the cartesian grid system and as 3D representation respectively. It can be seen that the superpotent spots occur towards the wall and the subpotent spots occur mainly near the central regions of the mixer. Also note that no superpotent or subpotent spots occur in the layer 4. This observation confirms hypothesis that

the NIR probe in its current location is unable to capture the variations that occur in the API 1 composition with respect to the other layers.

Similarly, Figures 4.6a and b present poorly mixed zones for API 2 in the Cartesian system and 3D representation respectively. The segregation pattern of API 2 is similar to that of API 1 (i.e., the superpotent and subpotent locations occur mainly towards the wall and the center respectively). Figures 4.7a and b give the bin locations for the extra granular phase in the Cartesian system and 3D representation respectively. For extra granular phase, the superpotent spots occur towards the center and the subpotent spots occur towards the wall. This implies that the extra granular phase is forming a slow mixing segregated layer near the center of the blender.

The zones identified in this study represent poorly mixed regions in the model. Thus they can be potential sampling sites to enable better estimation of variation in the blend.

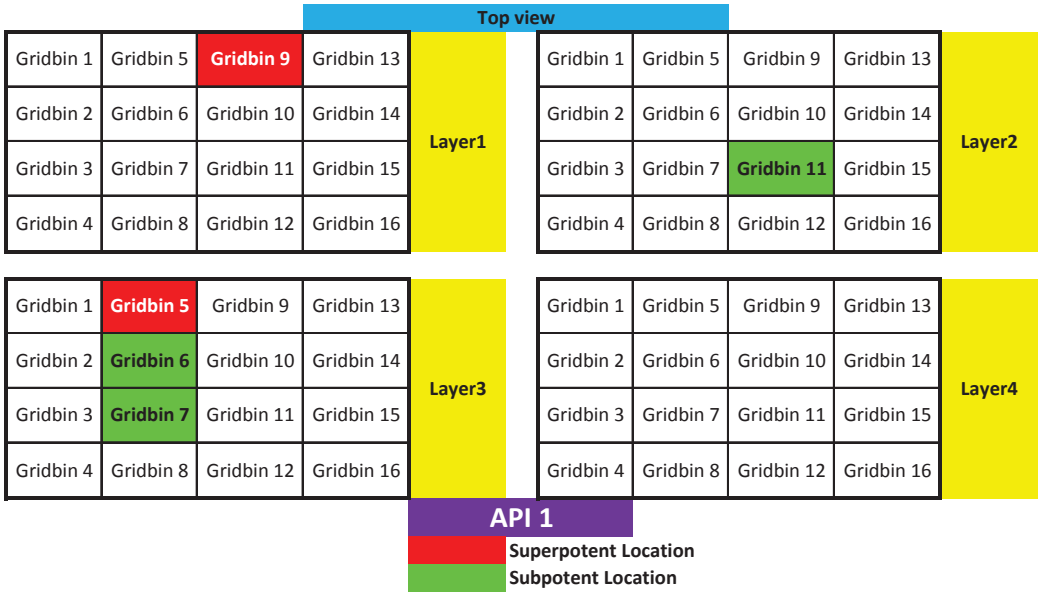

(a)

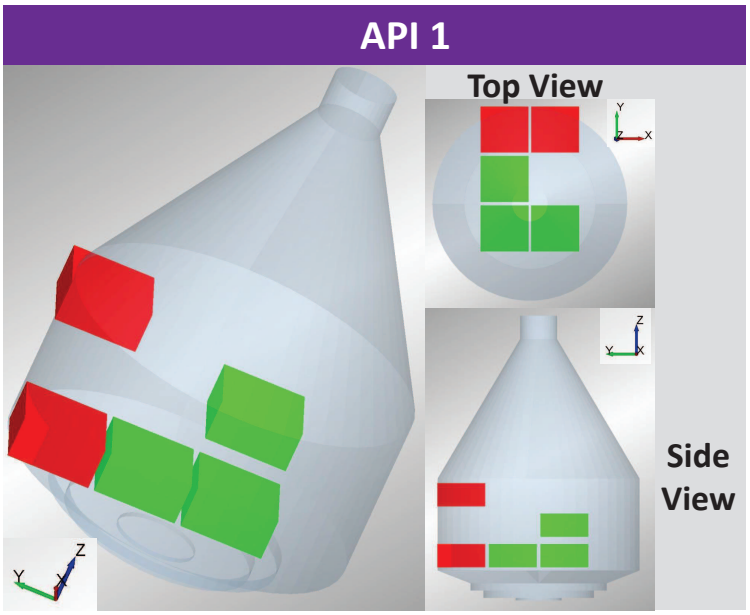

(b)

Figure 4.5: Superpotent and Subpotent regions in the mixing of API 1 represented as (a) Cartesian grid system (b) 3D representation

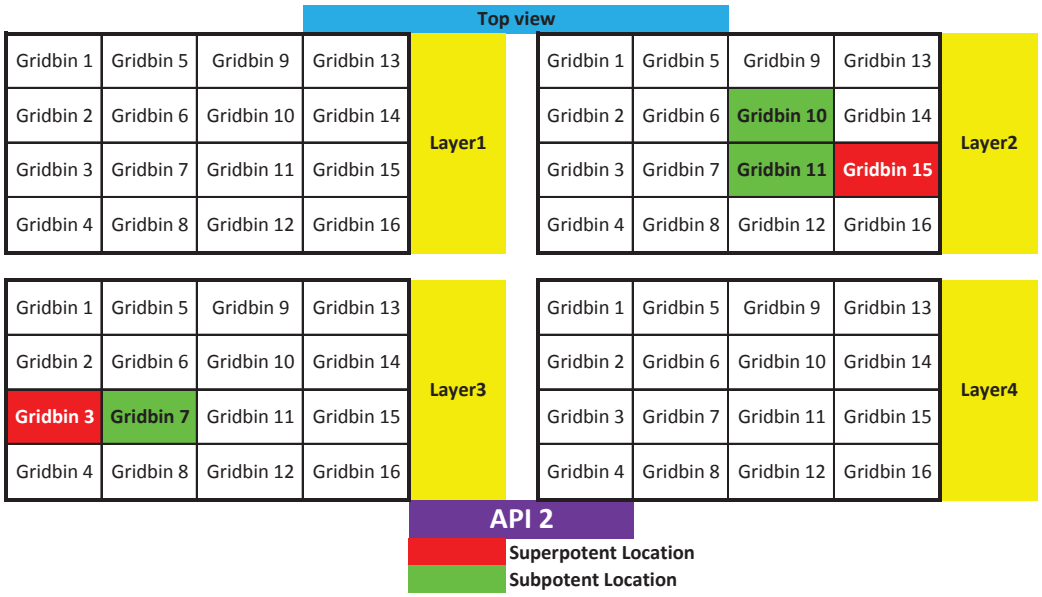

(a)

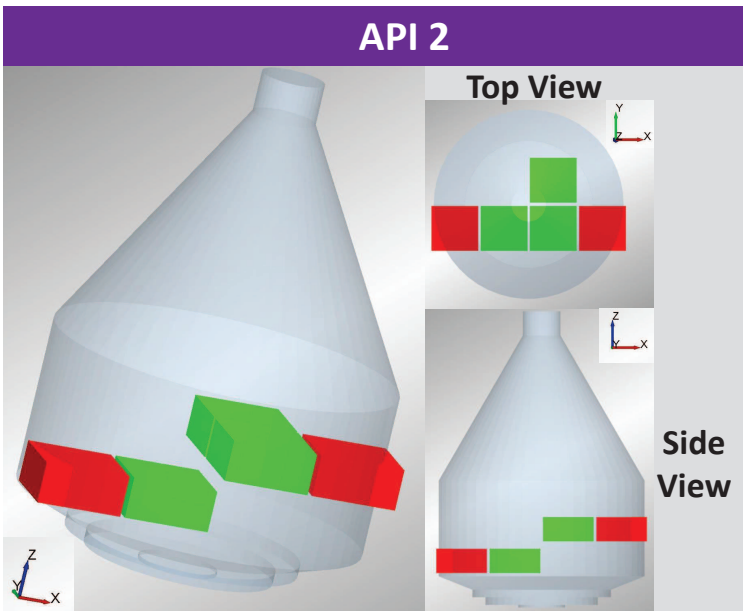

(b)

Figure 4.6: Superpotent and Subpotent regions in the mixing of API 2 represented as (a) Cartesian grid system (b) 3D representation

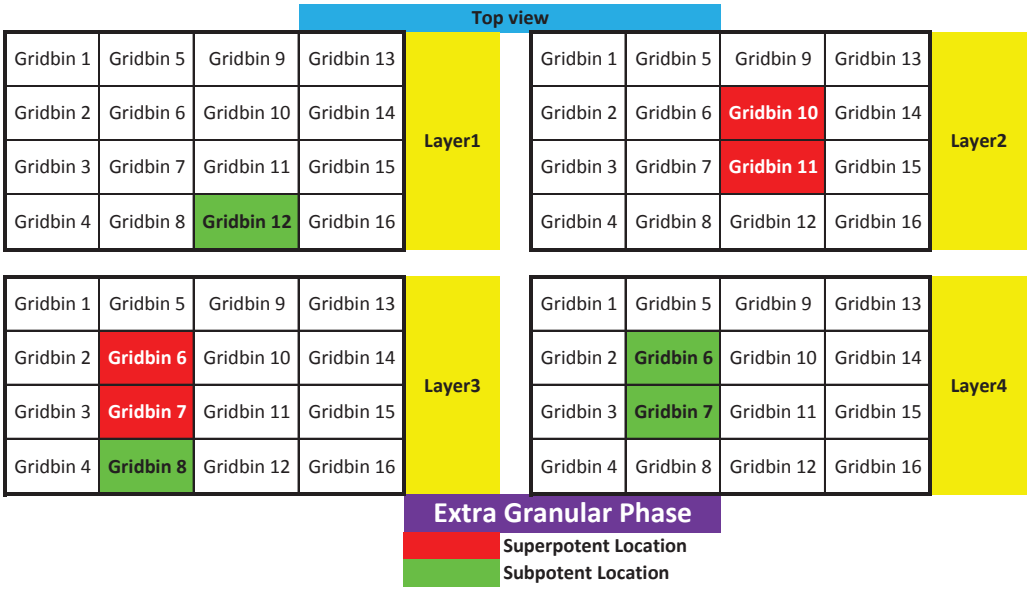

(a)

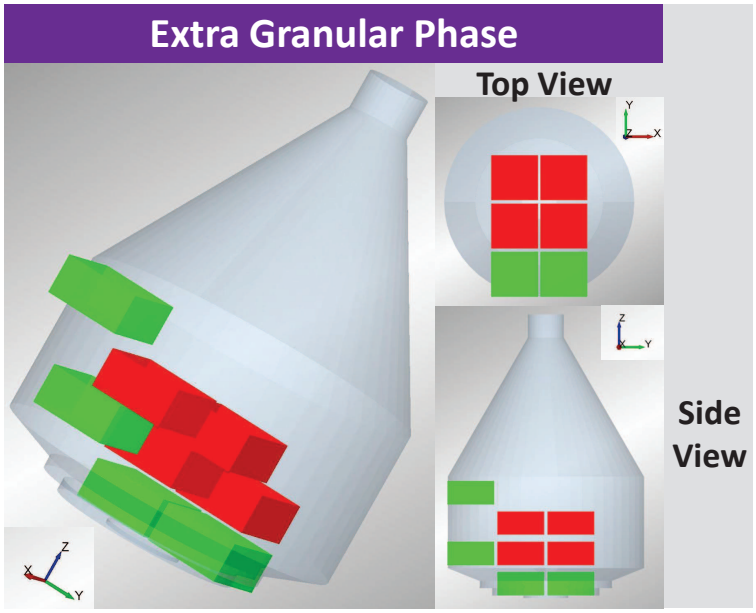

(b)

Figure 4.7: Superpotent and Subpotent regions in the mixing of Extra Granular Phase represented as (a) Cartesian grid system (b) 3D representation

4.5 Proposed sampling sites for determining RSD

As previously mentioned, the RSDs of API 1 and API 2 are being underestimated by calculations involving compositions captured in Layer-4 (NIR region). Underestimation of RSD is not beneficial as it deceives the quality of mixing of the batch. A poorly mixed batch could be judged as being well mixed and passed on to downstream operations and as a result the final product quality might be poor. Such an event could be very detrimental in pharmaceutical industries as the composition of API in tablets made from the same batch could be drastically different.

In order to get a better estimate of the RSD, additional sampling points have been proposed in this study. A new RSD has been calculated using grid bins in layer-4 close to NIR as well as the superpotent regions found from the previous study. The superpotent regions have been chosen as additional sampling points because they are close to the blender walls. It would be more practical to monitor these regions compared to central regions of the blender. This new RSD has been termed 'Wall hot-spot RSD' and has been compared in Figure 4.8 with the Overall RSD (which has been calculated with compositions from all but the excluded grid bins) and the layer-4 RSD (calculated using the grid bins close to NIR region). Figures 4.8 (a) and (b) show the variation of these RSD values with the number of revolutions for API 1 and API 2 respectively. It can be seen that inclusion of the superpotent sampling points in RSD calculations results in better estimation of the overall RSD of the mixture for both the compounds. However, these are results from a model based study and require further experimental verification before implementation. Note that this study was not conducted on the extra granular phase since the layer-4 RSD already provides a good estimate of the overall RSD as seen in figure 4.3 c.

4.6 Reducing Segregation Intensity of Extra Granular Phase

Segregation of the extra granular phase is an undesired effect in this mixing process. Therefore, certain process parameters critical to mixing (e.g., fill volume and RPM) have been varied and their effect on the mixing dynamics of the extra granular phase has been studied. This could lead to an understanding of how these CPPs have to be tuned in order to reduce the segregation intensity and thus eliminate the slow mixing center formed by the extra granular phase.

For this study two additional simulations have been conducted. In the first simulation the fill volume has been reduced to 40% (125,000 particles simulated). In the other one the blender RPM has been increased to 12 RPM. All other simulation parameters have been kept the same as in the base case.

Figure 4.9 shows the change in intensity of segregation of the extra granular phase with variation in RPM and fill level. It can be seen that the segregation intensity reduces with increase in RPM and decrease in fill level. As the RPM increases,the convective transport of the particles is increased. This results in faster and more efficient mixing. With decrease in fill level, segregation intensity decreases because the particles have more space to move and this aids particle transport. This observation also agrees with the previous studies available in literature [2, 30].

4.7 Effect of Critical process parameters

As identified in previous studies [31], the main design and process variables which affect the mixing dynamics are the design of the blender, the blender size, the mixing mechanism, the fill volume, rotation speed of the blender, material loading order and the material properties of the substances being blended. For this study, the design parameters, the equipment geometry and the material properties have been fixed while the process variables (i.e., the loading order and blender RPM)

have been varied in order to determine their effect on the mixing performance of this particular system. This study demonstrates how this model can be used for process design and optimization. The model can be used to determine the sensitivity of the parameters and the range in which the parameter values must be maintained in order to obtain the desired mixing performance. The mixing efficiency has been calculated based on the RSD of API 1 which has been determined based on equation (4.1).

A simulation has been run by increasing the RPM to 12 while keeping the other simulation parameters constant. In another simulation, the loading order has been varied. Figure 4.10 shows the two different loading orders (i.e., base case loading order and alternate loading order). In the alternate loading order simulation, the materials have been loaded in the following sequence: entire mass of API 2 followed by all of API 1 and lastly all of the extra granular phase.

Figure 4.11 presents the plot of RSD with respect to API 1 for alternate loading order, higher blender RPM. It can be seen that the effect of loading order is the least as the change in RSD with the alternate loading order is 0.5%. There is a 23.5% decrease in RSD when the blender RPM is doubled. The blender RPM has a considerable effect on the RSD, which implies that it is a sensitive CPP in the model. It can be seen from figure 4.11 that the RSD decreases with increase in RPM. As highlighted previously, this occurs due to increase in convective particle transport. The RSD increases with higher fill volume. This observation can be explained based on the fact that with increase in fill level, less free space is available for particle movement which hinders the particle transport. The other parameter of interest in batch mixing is the mixing time, which is also another important factor in deciding the blend quality [32]. Mixing time will change if the CPPs are varied. It can be adjusted to obtain the desired product quality. However in this work, a study on the mixing time has not been conducted, as the present DEM model is computationally intensive.

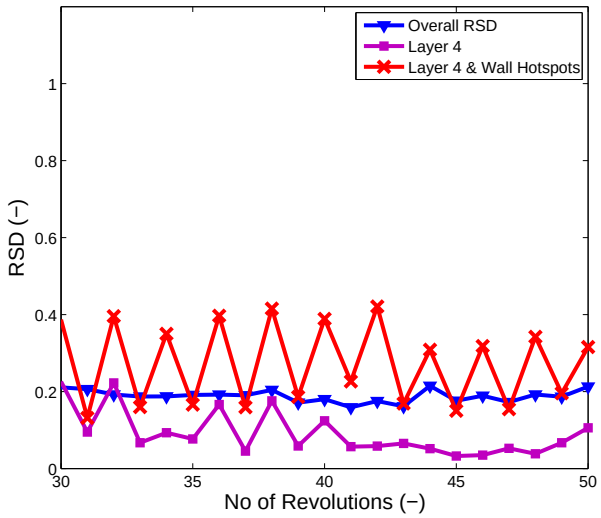

(a)

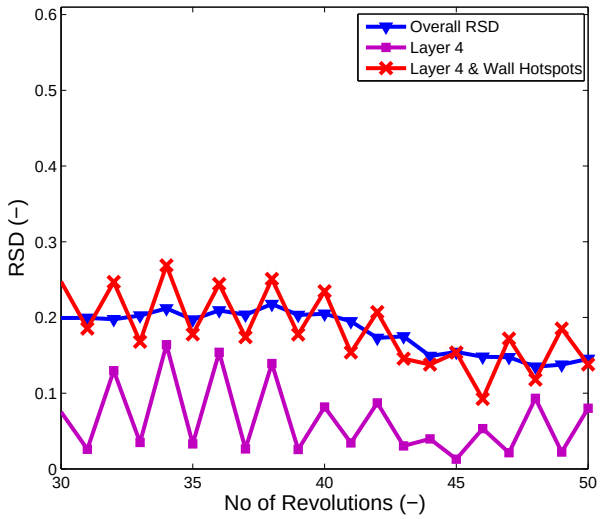

(b)

Figure 4.8: Comparison of Overall RSD with Layer-4 and Wall hotspots for (a) API 1 (b) API 2

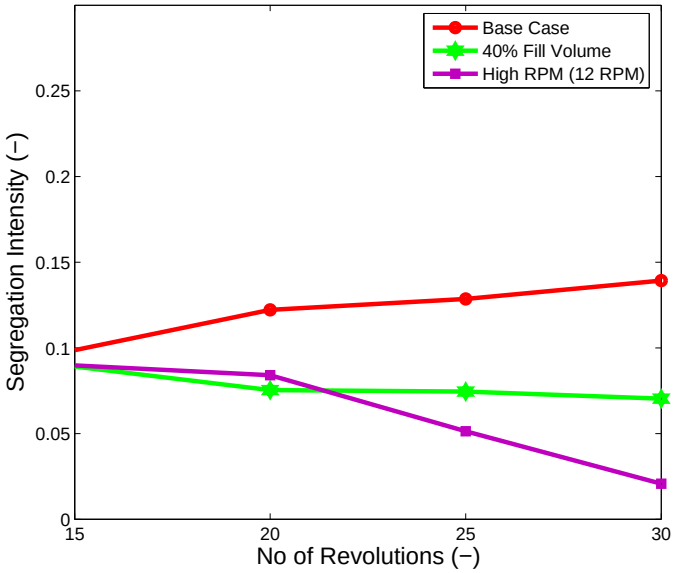

Figure 4.9: Variation of segregation intensity of Extra Granular Phase with change in processing conditions

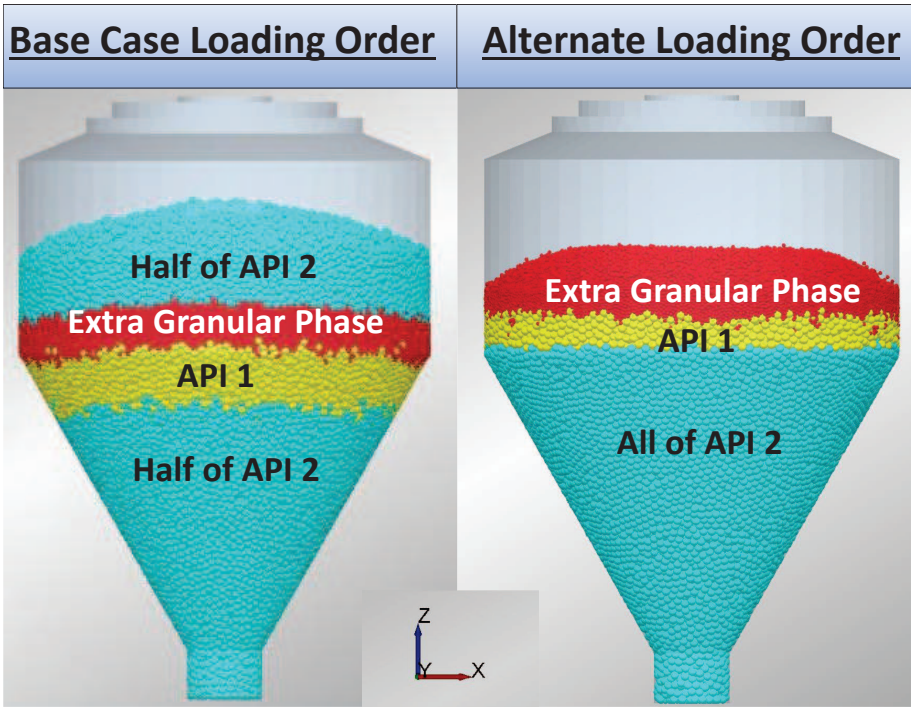

Figure 4.10: Loading order of the materials

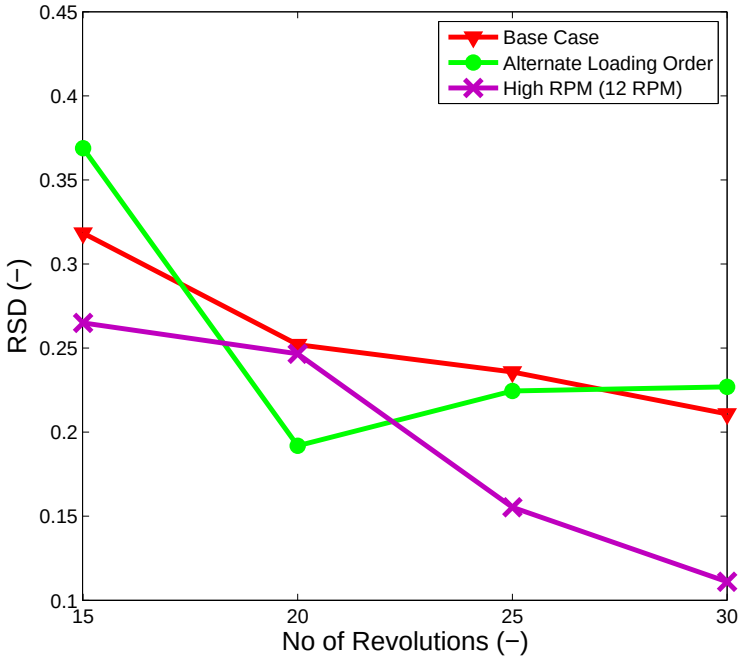

Figure 4.11: Variation of RSD of API 1 with change in processing condition

Chapter 5
Conclusions and Future work

A mathematical model for an industrial batch bin blender has been presented based on the DEM methodology. The model has been developed based on an experimental set-up and has been shown to capture the process dynamics well. The simulation parameters have been calibrated and tuned using experimental data. In the experimental set-up, a NIR probe located on the lid of the bin is used to obtain information about the composition of the mixture near the lid zone. However, the model has been used to evaluate the overall mixing performance. Since three types of raw materials with different physical properties and particle sizes are being mixed, a segregation study has also been conducted to highlight the segregation pattern of the different materials being mixed. The model has been used to determine other potential sampling sites by identifying the superpotent (i.e., where the material concentration is considerably higher than the overall average composition) and subpotent zones (i.e., where the material concentration is considerably lower than the overall average composition). The model has been used to identify additional sampling points that are able to improve the prediction of the overall RSD calculations but these points need to be experimentally verified. With the help of the model, alternate processing conditions have also been suggested for counteracting the segregation effect on the external granular phase. The intensity of segregation was found to decrease considerably with increase in blender RPM and decrease in fill volume. Hence this work provides an excellent demonstration of how model based methods can be used to study the process dynamics and aid the pharmaceutical industries in process design and optimization

as outlined in PAT. A separate study on the impact of different CPPs (blender RPM, fill volume and loading order) has been conducted as well. It is seen that the loading order is the least sensitive in this particular case whereas fill volume and blender RPM have high sensitivity towards the blend product quality.

The results obtained from this model have been shown to agree with previous studies reported in literature [2, 30, 31]. Similar framework/approach can be implemented to study the effect of blender geometry or equipment design parameters and different mixing mechanisms as well. Future work could involve the validation of the results using the experimental setup and improving the simulation speed of the present framework with the help of parallel computing tools as DEM models are computationally intensive in nature.

References

[1] M. Alian, F. Ein-Mozaffari, S. R. Upreti, Analysis of the mixing of solid particles in a plowshare mixer via discrete element method (DEM), Powder Technology 274 (2015) 77–87.

[2] P. E. Arratia, N. Duong, F. J. Muzzioa, P. Godbole, S. Reynolds, A study of the mixing and segregation mechanisms in the bohle tote blender via DEM simulations, Powder Technology 164 (2006) 50–57.

[3] F. Boukouvala, A. Dubey, A. Vanarase, R. Ramachandran, F. J. Muzzio, M. Ierapetritou, Computational approaches for studying the granular dynamics of continuous blending processes, 2-population balance and data-based methods, Macromolecular Materials and Engineering 297 (2012) 9–19.

[4] F. Boukouvala, Integrated simulation and optimization of continuous pharmaceutical manufacturing, Chemical and Biochemical Engineering Department (2013) Rutgers, The State University of New Jersey: New Brunswick, NJ.

[5] USFDA, Guidance for industry Q10 pharmaceutical quality system, H.a.H. Services (2004) Maryland.

[6] USFDA, Guidance for industry Q8(R2) pharmaceutical development, H.a.H. Services (2009) Maryland.

[7] B. Chaudhuri, A. Mehrotra, F. J. Muzzio, M. S. Tomassone, Cohesive effects in powder mixing in a tumbling blender, Powder Technology 165 (2006) 105–114.

[8] USFDA, Guidance for industry Q9 quality risk management, H.a.H. Services (2006) Maryland.

[9] A. Di Renzo, F. P. Di Maio, Comparison of contact-force models for the simulation of collisions in DEM-based granular flow codes, Chemical Engineering Science 59 (2004) 525–541.

[10] H. Kruggel-Emden, E. Simsek, S. Rickelt, S. Wirtz, V. Scherer, Review and extension of normal force models for the discrete element method, Powder Technology 171 (2007) 157–173.

[11] A. Dubey, A. Sarkar, M. Ierapetritou, C. R. Wassgren, F. J. Muzzio, Computational approaches for studying the granular dynamics of continuous blending processes, 1-DEM based methods, Macromolecular Materials and Engineering 296 (2011) 290–307.

[12] B. Remy, J. G. Khinast, B. J. Glasser, Discrete element simulation of free flowing grains in a four-bladed mixer, AIChE Journal 55 (2009) 2035–2048.

[13] A. Sarkar, C. Wassgren, Continuous blending of cohesive granular material, Chemical Engineering Science 65 (21) (2010) 5687 – 5698.

[14] P. M. Portillo, F. J. Muzzio, M. G. Ierapetritou, Using compartment modeling to investigate mixing behavior of a continuous mixer, Journal of Pharmaceutical Innovation 3 (2008) 161 – 174.

[15] D. Ponomarev, V. Mizonov, C. Gatumel, H. Berthiaux, E. Barantseva, Markov-chain modelling and experimental investigation of powder-mixing kinetics in static revolving mixers, Chemical Engineering and Processing: Process Intensification 48 (2009) 828–836.

[16] D. V. Khakhar, A. V. Orpe, J. M. Ottino, Continuum model of mixing and size segregation in a rotating cylinder: concentration-flow coupling and streak formation, Powder Technology 116 (2001) 232–245.

[17] M. Sen, R. Ramachandran, A multi dimensional population balance model approach to continuous powder mixing processes, Advanced Powder Technology 24 (2013) 51–59.

[18] P. Tahvildarian, F. Ein-Mozaffari, S. R. Upreti, Circulation intensity and axial dispersion of non-cohesive solid particles in a v-blender via dem simulation, Particuology 11 (2013) 619–626.

[19] M. Alian, F. Ein-Mozaffari, S. R. Upreti, J. Wu, Using discrete element method to analyze the mixing of the solid particles in a slant cone mixer, Chemical Engineering Research and Design 93 (2015) 318–329.

[20] X. Ren, J. Xu, H. Qi, L. Cui, W. Ge, J. Li, GPU-based discrete element simulation on a tote blender for performance improvement, Powder Technology 239 (2013) 348–357.

[21] H. Komossa, S. Wirtz, V. Scherer, F. Herz, E. Specht, Transversal bed motion in rotating drums using spherical particles: Comparison of experiments with DEM simulations, Powder Technology 264 (2014) 96–104.

[22] C. Ammarcha, C. Gatumel, J. L. Dirion, M. Cabassud, V. Mizonov, H. Berthiaux, Transitory powder flow dynamics during emptying of a continuous mixer, Chemical Engineering and Processing: Process Intensification 65 (2013) 68–75.

[23] M. Sen, D. Barrasso, R. Singh, R. Ramachandran, A multi-scale hybrid CFD-DEM-PBM description of a fluid bed granulation process, Processes 2 (2014) 89–111.

[24] M. Sen, A. Dubey, R. Singh, R. Ramachandran, Mathematical development and comparison of a hybrid PBM-DEM description of a continuous powder mixing process, Journal of Powder Technology (2013) DOI 10.1155/2013/843784.

[25] P. M. Portillo, F. J. Muzzio, M. G. Ierapetritou, Hybrid DEM-compartment modeling. approach for granular mixing, AIChE Journal 53 (2007) 119 – 128.

[26] R. Kumar, B. Freireich, C. Wassgren, DEM-compartment-population balance model for particle coating in a horizontal rotating drum, Chemical Engineering Science 125 (2015) 144–157.

[27] Y. C. Zhou, B. H. Xu, A. B. Yu, P. Zulli, An experimental and numerical study of the angle of repose of coarse spheres, Powder Technology 125 (2002) 45–54.

[28] A. Alexander, C. Goodridge, F. Muzzio, P. Arratia, D. Brone, O. Sudah, Characterization of the performance of bin blenders part 1 of 3: Methodology, Pharmaceutical Technology.

[29] P. V. Danckwerts, The effect of incomplete mixing on homogeneous reactions, Chemical Engineering Science 8 (1958) 93–102.

[30] O. S. Sudah, D. Coffin-Beach, F. J. Muzzio, Effects of blender rotation speed and discharge on the homogeneity of cohesive and free flowing mixtures, International Journal of Pharmaceutics 247 (2002) 57–68.

[31] P. M. Portillo, M. Ierapetritou, S. Tomassone, C. Mc Dade, D. Clancy, P. P. C. Avontuur, F. J. Muzzio, Quality by design methodology for development and scale-up of batch mixing processes, Journal of Pharmaceutical Innovation 3 (2008) 258–270.

[32] I. Gijon-Arreortua, A. Tecante, Mixing time and power consumption during blending of cohesive food powders with a horizontal helical double-ribbon impeller, Journal of Food Engineering 149 (2015) 144–152.